A Co-CRISPR Strategy for Efficient Genome Editing in *Caenorhabditis elegans*

Heesun Kim,*,†,1 Takao Ishidate,†,‡,1 Krishna S. Ghanta,*,† Meetu Seth,*,†,‡ Darryl Conte Jr.,*,† Masaki Shirayama,*,†,‡,2 and Craig C. Mello*,†,‡,2

*Program in Molecular Medicine, †RNA Therapeutics Institute, and ‡Howard Hughes Medical Institute, University of Massachusetts Medical School, Worcester, Massachusetts 01605

ABSTRACT Genome editing based on CRISPR (clustered regularly interspaced short palindromic repeats)-associated nuclease (Cas9) has been successfully applied in dozens of diverse plant and animal species, including the nematode *Caenorhabditis elegans*. The rapid life cycle and easy access to the ovary by micro-injection make *C. elegans* an ideal organism both for applying CRISPR-Cas9 genome editing technology and for optimizing genome-editing protocols. Here we report efficient and straightforward CRISPR-Cas9 genome-editing methods for *C. elegans*, including a Co-CRISPR strategy that facilitates detection of genome-editing events. We describe methods for detecting homologous recombination (HR) events, including direct screening methods as well as new selection/counter-selection strategies. Our findings reveal a surprisingly high frequency of HR-mediated gene conversion, making it possible to rapidly and precisely edit the *C. elegans* genome both with and without the use of co-inserted marker genes.

SEQUENCE-specific immunity mechanisms such as RNA interference (Voinnet 2001; Zamore 2001; Grishok and Mello 2002; Hannon 2002) and CRISPR (clustered regularly interspaced short palindromic repeats)-Cas9 (Horvath and Barrangou 2010; Bhaya *et al.* 2011; Terns and Terns 2011; Wiedenheft *et al.* 2012) provide sophisticated cellular defense against invasive nucleic acids. Understanding how these defense systems work has enabled researchers to redirect them at cellular targets, providing powerful tools for manipulating both gene expression and the cellular genome itself. The CRISPR-Cas9 system is a bacterial antiviral mechanism that captures fragments of viral DNA in specialized genomic regions for reexpression as small-guide RNAs (sgRNAs) (Bhaya *et al.* 2011; Terns and Terns 2011; Wiedenheft *et al.* 2012). In bacterial cells Cas9–sgRNA complexes provide acquired immunity against viral pathogens (Bhaya *et al.* 2011; Terns and Terns 2011; Wiedenheft *et al.* 2012). When coexpressed along with an artificial sgRNA designed to target a cellular gene, the Cas9 nuclease has been shown to efficiently direct the formation of double-strand breaks at the corresponding target locus (Jinek *et al.* 2012). Though bacterial in origin, this mechanism works efficiently even within the context of eukaryotic chromatin (Gilbert *et al.* 2013). Genome editing using CRISPR-Cas9 has recently been demonstrated in numerous organisms, providing a powerful new tool with rapidly growing—if not infinite—potential for diverse biological applications (Bassett *et al.* 2013; Chang *et al.* 2013; Cho *et al.* 2013a; Cong *et al.* 2013; Dicarlo *et al.* 2013; Dickinson *et al.* 2013; Feng *et al.* 2013, 2014; Friedland *et al.* 2013; Gratz *et al.* 2013; Jiang *et al.* 2013; Mali *et al.* 2013b; Wang *et al.* 2013; Ma *et al.* 2014; Yu *et al.* 2014; Zhou *et al.* 2014).

The CRISPR-Cas9 system has also been successfully applied to *Caenorhabditis elegans*. Methods that have been used to express Cas9 include mRNA injection and transgene-driven expression from a constitutive or an inducible promoter (Chen *et al.* 2013; Chiu *et al.* 2013; Cho *et al.* 2013b; Dickinson *et al.* 2013; Friedland *et al.* 2013; Katic and Grosshans 2013; Lo *et al.* 2013; Tzur *et al.* 2013; Waaijers *et al.* 2013; Zhao *et al.* 2014). The U6 promoter has been used to drive sgRNA expression (Chiu *et al.* 2013; Dickinson *et al.* 2013; Friedland *et al.* 2013; Katic and Grosshans 2013; Waaijers

doi: 10.1534/genetics.114.166389
Manuscript received April 15, 2014; accepted for publication May 21, 2014; published Early Online May 30, 2014.
Available freely online through the author-supported open access option.
Supporting information is available online at http://www.genetics.org/lookup/suppl/doi:10.1534/genetics.114.166389/-/DC1.
[1]These authors contributed equally to this work.
[2]Corresponding authors: RNA Therapeutics Institute, University of Massachusetts Medical School, 368 Plantation St., AS5-2011, Worcester, MA 01605. E-mail: masaki.shirayama@umassmed.edu; RNA Therapeutics Institute, University of Massachusetts Medical School, 368 Plantation St., AS5-2049, Worcester, MA 01605. E-mail: craig.mello@umassmed.edu

et al. 2013). The system has been used widely to produce small insertions and deletions (indels) that shift the reading frame of the target gene, often resulting in premature termination of translation and loss-of-function phenotypes (Chiu *et al.* 2013; Cho *et al.* 2013b; Friedland *et al.* 2013; Lo *et al.* 2013; Waaijers *et al.* 2013). In addition, single-strand oligonucleotides have been used as donor molecules to precisely alter a target gene through homologous recombination (HR) (Zhao *et al.* 2014), and a selection scheme has been developed that allows the HR-mediated insertion of large sequence tags such as GFP (Chen *et al.* 2013; Dickinson *et al.* 2013; Tzur *et al.* 2013).

Despite these important advances, current CRISPR protocols for inducing indels and HR events in *C. elegans* could benefit from refinement. For example, different sgRNAs targeting the same gene can result in substantially variable DNA cleavage efficiencies (Bassett *et al.* 2013; Chen *et al.* 2013; Wang *et al.* 2014); thus, identifying active sgRNAs can be time consuming and costly.

In this study, we investigate several strategies with which to streamline CRISPR-Cas9-mediated genome editing in *C. elegans*. We describe a Co-CRISPR strategy that can facilitate the identification of functional sgRNAs and can enrich for transgenic animals carrying an HR event. We show that HR events can be identified without the need for selection at a rate of ~1% to as high as 10% of F1 transgenic animals scored. This high frequency allows HR events to be identified by directly scoring for GFP expression or by PCR screening to detect HR-induced DNA polymorphisms. Direct screening allows precise genome alterations that minimize the footprint of DNA alterations, such as inserted selectable markers, at the target locus. However in some cases, such as whole-gene deletion assays that may induce lethality, selection can be useful for both identifying and maintaining HR events. We therefore describe a straightforward selection/counterselection protocol that facilitates recovery of HR events where having a marker inserted at the target site might be tolerated or useful. Together the findings presented here take much of the guesswork out of using the CRISPR-Cas9 system in *C. elegans*, and the Co-CRISPR strategy employed here may also prove useful in other organisms.

Materials and Methods

Genetics

All strains in this study were derived in the Bristol N2 background and maintained on nematode growth medium (NGM) plates seeded with OP50 (Brenner 1974).

Selection of sgRNA target sequences

We manually searched for target sequences consisting of $G(N)_{19}NGG$ (Wiedenheft *et al.* 2012; Friedland *et al.* 2013) near the desired mutation site. For HR-mediated repair experiments such as *gfp* knock-in and introduction of point mutation, we selected the target sequences where it was possible to introduce a silent mutation in the PAM site. Target sequences are listed in Supporting Information, Table S1.

Preparation of sgRNA constructs

We replaced the *unc-119* target sequence in pU6::unc-119 sgRNA vector (Friedland *et al.* 2013) with the desired target sequence using overlap extension PCR. The pU6::unc-119 sgRNA vector was diluted to 2 ng/μl and used as a template to generate two overlapping fragments. The first was amplified using the primers CMo16428 and sgRNA R, resulting in the U6 promoter fused to the GN_{19} target sequence (U6p::GN_{19}). The second was amplified using the primers CMo16429 and sgRNA F, resulting in the GN_{19} target sequence fused to the sgRNA scaffold and U6 3′-UTR. These two PCR products were mixed together, diluted 1:50, and used as a template for a PCR reaction with primers CMo16428 and CMo16429. The resulting pU6::target sequence::sgRNA scaffold::U6 3′-UTR fusion products were gel purified and inserted into the pCR-Blunt II-TOPO vector (Invitrogen, no. K2800-20). We used iProof high-fidelity DNA polymerase (Bio-Rad, no. 172-5300) in all PCR reactions above to minimize errors of PCR amplification, and all the constructs were confirmed by DNA sequencing. Primers sequences are listed in Table S2.

Preparation of HR donor vectors

***pie-1* donor plasmids (point mutations and *gfp* and *flag* fusions):** *pie-1* genomic sequence (LGIII:12,425,767-12,428,049) was amplified using the primers C_PIE-1 PF and C-PIE-1 PR and the resulting PCR product was inserted into the pCR-Blunt II-TOPO vector (Invitrogen, no. K2800-20).

The K68A and K68R mutations were introduced by PCR sewing (or overlap extension PCR). The *pie-1* plasmid described above was used as a template to generate overlapping PCR products with the corresponding site-specific mutations. The overlapping PCR products were mixed together (1:1), diluted 50-fold with water, and used as a template in the PCR-sewing step with an external primer pair. The fused PCR products were gel purified and cloned into the pCR-Blunt II-TOPO vector.

For building *gfp*::*pie-1* donor constructs, an *Nhe*I restriction site was inserted immediately after and in frame with the start codon of *pie-1* by PCR sewing. A plasmid containing wild-type or mutant *pie-1* sequence was used as a template to generate a left-arm PCR product flanked by *Bsi*WI and *Nhe*I restriction sites and a right-arm PCR product flanked by *Nhe*I and *Ngo*MIV restriction sites. The products were digested with *Nhe*I, purified using a PCR cleanup kit, and ligated together. The ligated products were cloned into the pCR-Blunt II-TOPO vector, and plasmids containing the appropriately ligated fragments were identified. A *Bsi*WI and *Ngo*MIV fragment, containing the in frame *Nhe*I site immediately after the start codon, was released and ligated to similarly digested *pie-1* constructs. The GFP coding region amplified from pPD95.75 (Addgene) was inserted into the *Nhe*I site.

For *pie-1*::*gfp* or *pie-1*::*flag*, a 1.6-kb fragment (LGIII 12,428,172–12,429,798) was amplified from genomic DNA and inserted into the pCR-Blunt II-TOPO vector (Invitrogen, no. K2800-20). Overlap extension PCR was used to introduce an *Nhe*I site immediately before the stop codon in this fragment of *pie-1*. A *3*×*flag* sequence (gattacaaagaccatgatggt gactataaggatcatgatattgactataaagacgatgacgataag) was inserted into the *Nhe*I site.

Finally, we used PCR sewing to introduce silent mutations that disrupt the PAM site (NGG to NTG) in each HR donor. The above plasmids were used as templates to generate the initial PCR products for PCR sewing. The final products were cloned into the pCR-Blunt II-TOPO vector.

We used iProof high-fidelity DNA polymerase (Bio-Rad, no. 172-5300) in all PCR reactions above. Primers are listed in Table S3.

mCherry::vet-2 and flag::vet-2 donor construct: A 2411-bp DNA fragment of the *vet-2* gene, including 1249 bp of sequence upstream and 1162 bp downstream of the *vet-2* start codon (corresponding to the genomic sequence LGI:10,845,543-10,847,953), was amplified from genomic DNA and inserted into pBluescript KS (+) vector (Addgene). An *Xma*I site was introduced by PCR immediately after the *vet-2* start codon. The *mcherry* coding sequence amplified from pCFJ90 (Addgene) or 3×*flag* sequence was inserted into the *Xma*I site.

smo-1::flag donor plasmid: *smo-1* genomic sequence (LGI: 1,340,243–1,341,558) was amplified from N2 genomic DNA and inserted into the pCR-Blunt II-TOPO vector (Invitrogen, no. K2800-20). Overlap extension PCR was used to introduce an *Nhe*I site immediately before the stop codon in this fragment of *smo-1*. The resulting PCR product was cloned into the pCR-Blunt II-TOPO vector. A 3×*flag* fragment with *Nhe*I overhangs was generated by annealing two overlapping oligonucleotides and ligated into the *smo-1* donor plasmid. We mutated the PAM site (Figure S3C) as described for the *pie-1* donors above.

gfp::pie-1 for MosSCI: A 3744-bp fragment (*Sca*I–*Not*I) containing the *pie-1* promoter was excised from pID3.01B (Addgene) and inserted into a modified MosSCI LGII vector (B1496) in which a *Not*I site was added to pCFJ151 (Frokjaer-Jensen *et al.* 2008; Shirayama *et al.* 2012). A 2631-bp PCR fragment containing the *pie-1* open reading frame (ORF) and 3′-UTR was then inserted into the resulting plasmid to make a *gfp*::*pie-1* plasmid for MosSCI. The plasmid was injected into the strain EG4322 at a concentration of 10 ng/μl by direct injection method to insert a single-copy *gfp*::*pie-1* transgene on chromosome II at position 8,420,159.

BSD-fusion to pie-1: The nucleotide sequence of the Blasticidin S resistance gene (*BSD*) from *Aspergillus terreus* was codon optimized for *C. elegans* and an artificial intron (gtaagagatttttttaaaaatttatttttttacactgttttttctcag) was inserted into the middle of the *BSD* ORF: the entire gene was *de novo* synthesized by GenScript. The *BSD* fragment containing the *BSD* ORF (439 bp), *rpl-28* promoter (568 bp), and *rpl-28* 3′-UTR (568 bp) was inserted into pBluescript KS (+) vector (Addgene). The complete sequence of *BSD* marker is available upon request. A 1077-bp fragment of *pie-1* left homology was inserted into the *Xba*I site before the *rpl-28* promoter and a 1017-bp fragment of *pie-1* right homology was inserted into the *Sal*I–*Apa*I site after the *rpl-28* 3′-UTR. Blasticidin S (AG scientific, no. B-1247) was used to select animals transformed with the *BSD* gene.

cb-unc-119(+) donor plasmid: *Cbr-unc-119(+)* (2216 bp) was amplified from pCFJ151 (Frokjaer-Jensen *et al.* 2008; Shirayama *et al.* 2012) using primers tailed on the 5′ end and the 3′ end with the *loxP* (ataacttcgtataatgtatgctatac gaagttat) sequence (Dickinson *et al.* 2013). This *loxP*::*Cbr-unc-119(+)*::*loxP* fragment was inserted into pBluescript-KS(+) vector (Addgene) linearized with *Xho*I. A 1006-bp fragment of the sequence upstream of the *oma-1(tm1396)* deletion (LGIV: 8,884,663-8,891,662) was inserted into the *Spe*I site on one side of the *loxP*::*Cbr-unc-119(+)*::*loxP* cassette, and a 1000-bp fragment of the sequence downstream of the *oma-1(tm1396)* deletion (LGIV:8,887,927-8,894,926) was inserted into the *Apa*I site after the *loxP* site.

Preparation of heat-shock-Cas9 plasmid

The *Mos1* transposase ORF in pJL44 (Addgene) was replaced with Cas9 from *Peft3*::*Cas9* vector (Friedland *et al.* 2013) to generate *hs*::*Cas9* (pWU34) construct.

Micro-injection

DNA mixtures were micro-injected into the gonads of young adult worms. Plasmids for injection were prepared using a midiprep plasmid purification kit (Qiagen, no. 12143). For Co-CRISPR, we injected 50 ng/μl each vectors [Cas9 vector, *unc-22* sgRNA vector (Co-CRISPR), two untested-sgRNAs, and pRF4::*rol-6(su1006)*] (Figure 2A). Micro-injection mixtures for HR contained 50 ng/μl each Cas9 vector, sgRNA vector, pRF4::*rol-6(su1006)*, and HR donor vector. The final concentration of DNA in the injection mix did not exceed 200 ng/μl. For injection mixes with five different plasmids, 40 ng/μl of each plasmid was added. For HR experiments, we injected 40–60 worms and for disruptions, 20–30 worms. After recovering from injection, each worm was placed onto an individual plate.

Screening for indels using Co-CRISPR

To validate untested sgRNAs we injected mixtures containing the *unc-22* sgRNA and up to several untested sgRNAs (as described above). Three days after injection, F1 rollers and F1 twitchers were picked individually to plates and allowed to produce F2 progeny for 2–3 days. F1 twitchers and F1 rollers with twitching F2 progeny were then transferred to 20 μl lysis buffer for PCR, PAGE

(see below), and/or DNA sequencing analysis. Total time from injection to indel detection was ~6–7 days.

Screening for HR events

Direct detection of GFP: This procedure works for donor vectors that cannot drive GFP without first integrating into the genomic target site. For GFP::PIE-1 it was necessary to mount gravid F1 rollers three at a time under coverslips on 2% agarose pads for screening at 40× magnification using a Zeiss Axioplan2 microscope. For bright GFP constructs, it should be possible to screen using a fluorescence dissecting scope. GFP-positive animals were recovered by carefully removing the coverslip and transferring to individual plates. After laying eggs for 1 day they were individually lysed in 20 μl lysis buffer for PCR confirmation of the GFP insertion. GFP-positive F2 homozygotes were then identified and correct insertion of GFP was confirmed by DNA sequencing. Total time from injection to recovery of heterozygotes was 3–4 days.

PCR detection: F1 rollers were picked individually to plates and allowed to lay eggs for 1 day. For the Co-CRISPR assay, F1 rollers were allowed to produce F2 progeny for 2–3 days so that F2 twitcher progeny could be identified. (Note that F1 roller animals that segregate twitching progeny should be selected as these animals exhibit the highest HR frequency, while nonrolling F1 twitchers should be avoided; see *Results and Discussion*). F1 animals were then transferred into lysis buffer in indexed PCR tubes and were screened using primers outside the homology arms followed by restriction enzyme digestion to detect the insertion. In some experiments, 1 μl of the initial PCR reaction was used as a template for a second PCR reaction with primers within the donor sequences. Although useful, this latter procedure gave several false positives in our hands. Total time from injection to recovery of heterozygotes was 4 days. For the Co-CRISPR strategy, 3 more days were required to recover heterozygotes.

Selection/counterselection method: Four days after injection, gravid F1 rolling adults were placed in groups of 10–15 animals per plate onto media containing ivermectin and blasticidin (Figure 4B). After 3–4 more days, the plates were scored for viable, fertile progeny. Insertion of *BSD* at the target locus was then confirmed by PCR and DNA sequencing (as described above). The total time from injection to recovery of HR events was 7–10 days. Although slightly longer in duration this procedure required ~10 times less labor as only the relatively rare viable populations were subject to PCR and DNA sequence analysis. For donor molecules containing the *Cbr-unc-119(+)* selection, the procedure was essentially the same; however, blasticidin was omitted from the selective media and the recipient strain was both *Cbr-unc-119* mutant and ivermectin resistant. Primers for screening HR events are listed in Table S3.

Imaging

Images were captured with an ORCA-ER digital camera (Hamamatsu) and AxioVision (Zeiss) software.

Screening for small indels by PCR and PAGE

We designed primers to amplify (~30 cycles) PCR products of 60–65 bp encompassing the CRISPR-Cas9 target site. PCR products were resolved on 15% polyacrylamide gels to distinguish dsDNA molecules that differ by as little as 1 bp. We found that we could screen for indels even in HR experiments, but it required two PCR steps. In the first PCR reaction (~20 cycles), primers outside of the homology arms were used to avoid amplifying the donor sequence. In the second reaction (~15 cycles), 1 μl of the first PCR reaction was used as a template to generate the 60- to 65-bp PCR product encompassing the CRISPR-Cas9 target site. *TaKaRa Ex Taq* (Takara, no. RR001) was used for the PCR reactions above. Primer sequences are listed in Table S3.

Immunoblotting

One hundred adult worms were lysed in 80 μl of 1× sample buffer (25 μl of M9 containing 100 worms, 25 μl of 2× lysis buffer, 20 μl of 4× NuPAGE LDS Sample buffer (Invitrogen, no. NP0008), and 10 μl of β-mercaptoethanol by boiling for 20 min, freezing, and boiling again for 10 min. The worm lysate proteins were separated on 4–12% NuPAGE Tris–acetate Mini Gels (Invitrogen, no. NP0335BOX). Proteins were transferred to Immun-Blot PVDF Membrane (Bio-Rad, no.162-0177) at 100 V for 1 hr at 4°. Mouse monoclonal anti-PIE-1 antibody (P4G5) (Mello *et al.* 1996) and rabbit polyclonal anti-PGL-1 antibody was used at 1:50 and 1:500, respectively.

Results and Discussion

Using a visible cotransformation marker enriches for genome-editing events

While conducting CRISPR-Cas9 experiments to induce mutations in the *pie-1* gene, we used the dominant co-injection marker *rol-6* to monitor injection quality. From 60 injected animals, we obtained 93 fertile F1 rollers. Remarkably, we noted that several of these F1 rollers (5/93) produced 100% dead embryos exhibiting the distinctive *pie-1* maternal-effect embryonic lethal phenotype (Mello *et al.* 1996) (Figure 1A). Genomic sequencing of these F1 adults identified lesions in the *pie-1* gene consistent with Cas9-directed cleavage (Figure 1B). In some cases the maternal and paternal alleles exhibited distinct lesions, while in others, the same lesion was found in both alleles (Figure 1B). Since the DNA was delivered into the ovary of an adult, after the switch from sperm to oocyte development, the paternal allele must have been targeted in the F1 zygote soon after fertilization. The fact that both alleles exhibit identical lesions in some animals suggests that a chromosome previously cut by Cas9 and repaired by non-homologous end joining (NHEJ) was used as a donor molecule to copy the lesion into the homolog.

If the activation of Cas9 in the germline is broadly or nonspecifically mutagenic, then some injected animals would

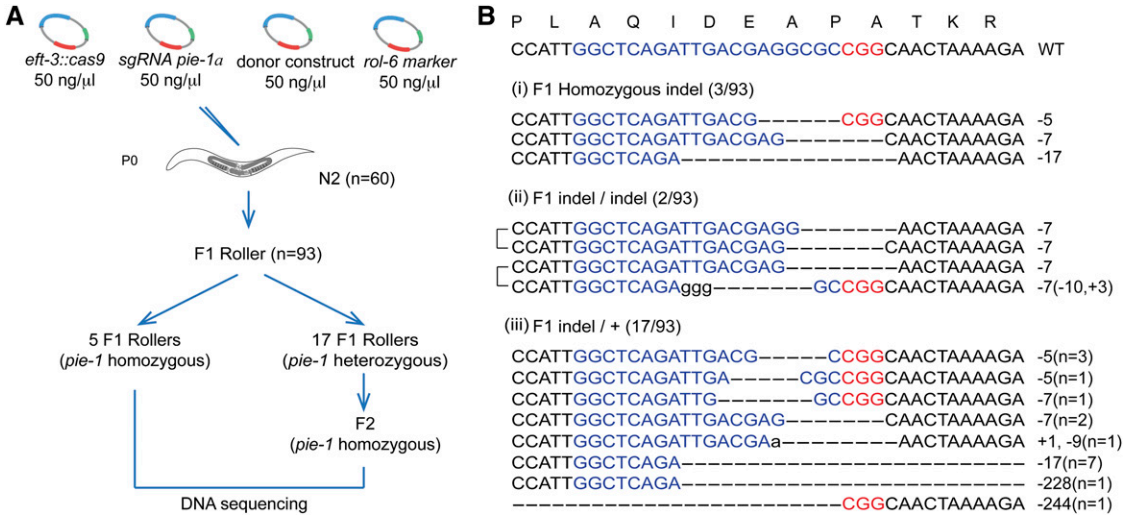

Figure 1 Efficient CRISPR-Cas9-mediated gene disruption in transgenic animals. (A) Schematic of screen for CRISPR-Cas9 genome editing events. The dominant transformation marker *rol-6* was co-injected with Cas9, *pie-1a* sgRNA, and donor plasmids. F1 rollers were screened for NHEJ-mediated indels by DNA sequencing. Among 93 F1 rollers, 22 indels were obtained. (B) Sequences of the wild-type *pie-1* target site (top) and CRISPR-Cas9-mediated indels among F1 animals: (i) *pie-1* homozygotes carrying the same indel on both alleles; (ii) *pie-1* homozygotes carrying a different indel on each allele; and (iii) *pie-1* heterozygotes. Lowercase letters indicate insertions, and dashes indicate deletions. The PAM is marked in red, and target sequences are marked in blue. The number of deleted (−) or inserted (+) bases is indicated to the right of each indel. The numbers in parentheses in (iii) represent the number of animals with the indels shown.

be expected to segregate novel mutants, including mutants with non-*pie-1* dead-embryo phenotypes. To look for evidence of off-target mutagenesis, we screened among the progeny of F1 rollers for animals producing dead embryos, or other visible phenotypes. A careful examination of F2 and F3 populations revealed 17 populations from 93 F1 rollers that segregated numerous dead embryos (Figure 1A). However, examination of these dead embryos by Nomarski microscopy revealed the distinctive *pie-1* mutant phenotype and no other phenotypes. Each of these 17 strains segregated *pie-1* homozygotes at the expected Mendelian frequency, indicating that the original F1 rollers were heterozygous for *pie-1* loss-of-function mutations. Sequencing of these strains revealed indels in the region of the *pie-1* gene targeted by CRISPR-Cas9 (Figure 1B). In some cases, to avoid the delay and added cost of DNA sequencing, genomic DNA prepared from lysates of each candidate was amplified as ~60-bp PCR products that were then analyzed on a 15% PAGE gel. This analysis easily detected lesions as small as 5 nt (Figure 1B and Figure S1A).

In addition to F1 rollers, we randomly selected F1 nonroller sibling progeny that were produced during the same time window as the F1 rollers. Among 100 nonroller siblings, we failed to find animals segregating dead embryos. Thus, using the dominant visible *rol-6* marker to identify F1 transgenic animals (rollers) also identified animals in which Cas9 was active. It is important to note, however, that very few of the animals with *pie-1* mutations continued to exhibit the roller phenotype in subsequent generations, suggesting that the *rol-6* transgene expression was transient and present only in the F1 generation.

A Co-CRISPR strategy to detect genome-editing events

In practice, we have found that about half of sgRNAs tested are not effective. Thus, while the *rol-6* marker was clearly useful for finding animals with CRISPR-Cas9-induced lesions, we nevertheless frequently had to screen through dozens or even hundreds of F1 rollers by PCR or sequencing only to conclude that CRISPR-Cas9 was not active in the injection. We therefore reasoned that co-injecting a proven sgRNA (one that works well and results in an easily recognized visible phenotype) would allow us to more directly identify animals in which Cas9 is active. We tested this strategy using an sgRNA targeting the muscle structural gene *unc-22* (Moerman and Baillie 1979; Benian *et al.* 1993). We chose this sgRNA both because *unc-22* loss of function causes a distinctive recessive paralyzed twitching phenotype that is easy to score and because this sgRNA works moderately well compared to other sgRNAs (Table S1). Thus, F1 and F2 *unc-22* twitchers should arise from animals exposed to the greatest levels of Cas9 activity and should therefore also have active Cas9 loaded with the co-injected sgRNAs.

To test the Co-CRISPR strategy, we co-injected the *unc-22* sgRNA with two previously validated sgRNAs targeting *avr-14* and *avr-15* (Figure 2A), two genes whose wild-type activities redundantly confer sensitivity to the potent nematicide ivermectin (Dent *et al.* 2000). The *rol-6* marker was also included in these injections to facilitate the identification of twitchers that arise in the F2 among the progeny of F1 roller animals. We then measured, among 55 F1 rollers, the frequency of ivermectin-resistant strains (20%, $n = 11$) and twitcher strains (11%, $n = 6$) (Figure 2A). Strikingly, selecting

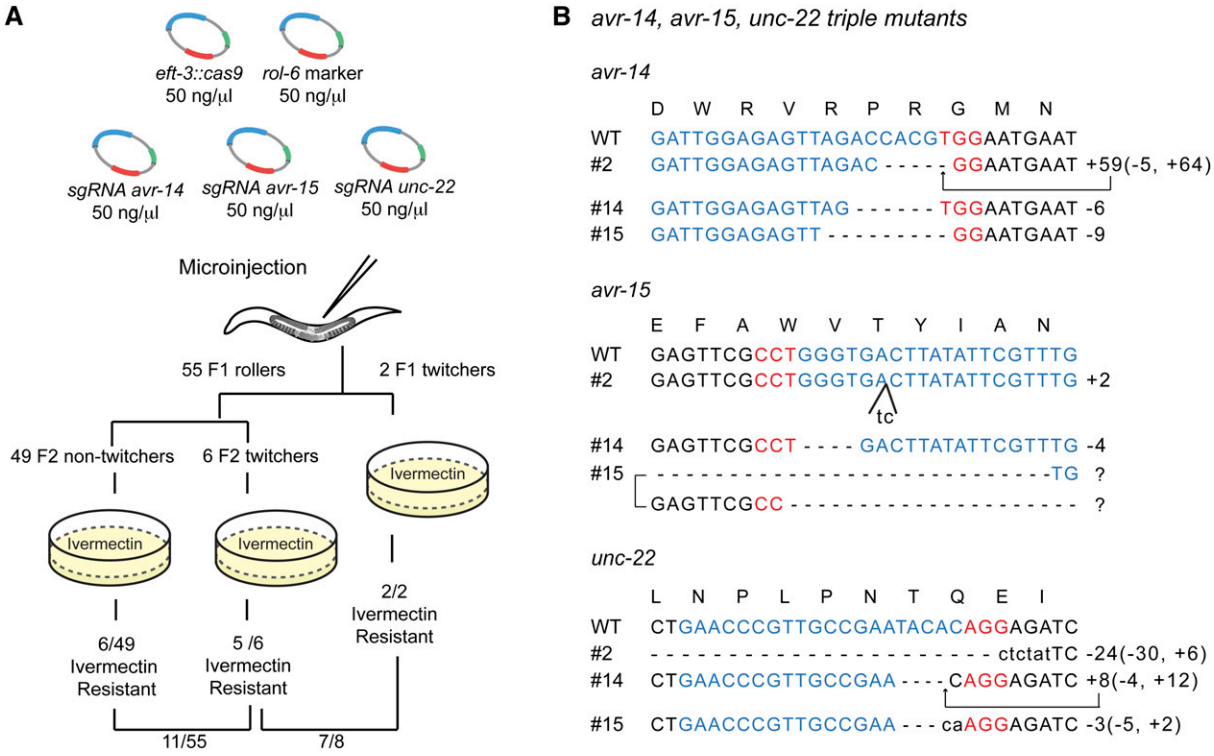

C

Gene	Number Injected	F1 rollers producing F2 twitchers/Total F1 rollers	F1 having both rolling and twitching phynotype	F1 twitchers	Roller-based indel frequency	Twitcher-based indel frequency
avr-14 *avr-15*	20	6/55	0	2	11/55 (20%)	7/8 (88%)
pie-1 b *pie-1* c	30	2/31	1	8	2/32 (6%) 1/32 (3%)	6/11(55%) 4/11(36%)

Figure 2 "*unc-22*" Co-CRISPR as a marker to indicate actively expressed Cas9. (A) Schematic of Co-CRISPR strategy to identify functional sgRNAs targeting *avr* genes. sgRNAs targeting *avr-14* and *avr-15* were co-injected with a functional *unc-22* sgRNA, the Cas9 expression vector, and the *rol-6* transformation marker. F1 rollers or twitchers were transferred to individual plates. The plates were allowed to starve, and then they were copied to plates containing 2 ng/ml ivermectin to identify CRISPR-Cas9-induced *avr-14*; *avr-15* double mutants. (B) Indel sequences in *avr-14*; *unc-22*; *avr-15* triple mutants. *avr-15* isolate 15 carried different indels on each allele. Sequences labeled with a question mark could not be precisely determined. (C) Comparison of twitcher-based indel frequency and roller-based indel frequency.

for the twitching phenotype dramatically enriched for animals exhibiting ivermectin resistance. For example, among 8 F1 animals that were either twitching themselves or produced twitcher progeny, 7 (88%) also produced progeny resistant to ivermectin (Figure 2, A and C). We confirmed Co-CRISPR activity by sequencing the lesions in several of these strains (Figure 2B).

Similar results were obtained in several additional Co-CRISPR experiments (Figure 2C and data not shown). For example, we used this approach to test two uncharacterized sgRNAs targeting the 3′ end of *pie-1* (Figure 2C and Figure S1B). Among 11 twitcher lines identified in the F1 or F2, we identified three indels by PCR and PAGE for one of the two sgRNAs (Figure S1B) and a single indel for the other sgRNA (Figure S1C). Sequence analysis confirmed these indels, which included a 6-nt deletion, a 24-nt insertion, and an 11-nt deletion for one sgRNA and a 16-nt insertion for the other. However, the PAGE detection method clearly underestimated the frequency of indels. Sequence analysis identified three heterozygous deletion mutations of 42, 43, and 603 nt that deleted primer binding sites and were thus too large to be detected by our PCR and PAGE analysis (Figure S1B). These unusually large deletions may reflect simultaneous cutting induced by the two adjacent sgRNAs whose targets are separated by 61 bp in this experiment (Figure S1B). In conclusion, these findings suggest that PAGE analysis of 10–20 Co-CRISPR lines should be sufficient to determine if an uncharacterized sgRNA is active. It should be

noted that since many F1 rollers analyzed were heterozygous for *unc-22* lesions, it was usually possible to find non-Unc segregants with an indel in the co-targeted gene using the *unc-22* Co-CRISPR assay. However, if *unc-22* is inconvenient for a particular experiment, our findings suggest that alternative Co-CRISPR sgRNAs targeting, for example, genes that when mutated confer resistance to ivermectin or benomyl or other genes with visible mutant phenotypes may be substituted (Table S1).

The observation that using nearby sgRNAs can induce deletions that remove the intervening sequence is consistent with previous findings in which large deletions were produced in this way (Horii *et al.* 2013; Ran *et al.* 2013; Ren *et al.* 2013; Wang *et al.* 2013; Zhou *et al.* 2014). Thus the Co-CRISPR strategy should facilitate the identification of deletions that remove the interval between two sgRNAs. However, further experimentation will be required to determine how large an interval can readily be eliminated. For the purpose of validating sgRNAs, our findings suggest that large deletions produced by testing multiple nearby sgRNAs simultaneously may confound the analysis of which sgRNAs are active. On the other hand, pooling sgRNAs targeting a number of different genes that are distant from one another in the genome should, in principle, allow several sgRNAs to be validated in a single Co-CRISPR micro-injection experiment.

Identification of HR events without a coselectable marker

We next sought to use CRISPR-induced double-strand breaks to drive HR. Several types of editing are possible, ranging from changing a single amino acid to inserting a protein tag such as GFP, or even deleting the entire target gene. In designing donor molecules to introduce point mutations or epitope fusions, we found it necessary to alter the sgRNA target sequence in the donor by mutating the protospacer adjacent motif (PAM) site or by introducing mismatches within the seed region (Jinek *et al.* 2012; Cong *et al.* 2013; Jiang *et al.* 2013; Sternberg *et al.* 2014). In our experience, failure to take this step frequently results in HR events containing CRISPR-Cas9-induced indels or a very low frequency of HR events, sometimes 0% (data not shown).

Previous studies successfully used single-strand oligonucleotide donor molecules (Zhao *et al.* 2014) or double-strand plasmid donor molecules (Dickinson *et al.* 2013) to induce HR events in *C. elegans*. However these studies relied on screening for a selectable phenotype introduced by the HR event. Given the high frequencies of NHEJ events detected in the studies above, we wondered if CRISPR-Cas9-mediated HR events could be recovered directly without the need for selection.

To test this idea, we decided to use CRISPR-Cas9-mediated HR to introduce the *gfp* coding sequence immediately downstream of the start codon in the endogenous *pie-1* locus (Figure 3A). The donor plasmid in this experiment contained *Nhe*I restriction sites flanking the *gfp* coding sequence, 1-kb homology arms, and a silent mutation that disrupts the PAM sequence at the sgRNA target site (Figure 3A). We generated three different donor constructs: *gfp*::*pie-1(WT)*, *gfp*::*pie-1(K68A)*, and *gfp*::*pie-1(K68R)*. Each donor molecule was co-injected with vectors to express the sgRNA, Cas9, and *rol-6* marker. We then directly examined the resulting F1 rolling animals for GFP::PIE-1 expression in the germline and embryos using epifluorescence microscopy (Figure 3B, see *Materials and Methods*). Using this approach, we obtained 9 independent gfp::pie-1(K68A) lines from 92 F1 rollers, 1 gfp::pie-1(K68R) line from 69 F1 rollers, and 1 gfp::pie-1(WT) line from 72 F1 rollers. Subsequent analyses revealed that each of these F1 animals was heterozygous for *gfp*::*pie-1*, and each strain incorporated both the *gfp* coding sequence and the PAM site mutation, as well as the linked K68A and K68R missense mutations. For unknown reasons, we found that one of the nine *gfp*::*pie-1(K68A)* lines could not be maintained.

The high rates of HR observed in the above study suggested that it should also be possible to recover HR events by screening DNA isolated from F1 rollers using PCR. To test this idea, we designed donor molecules to insert the *pie-1* lysine 68 lesions without tag sequences (Figure S2A) or to insert sequences encoding the FLAG epitope immediately before the stop codon of the *pie-1* gene (Figure 3F). For these HR experiments, we used 300 bp (no tag) and 800 bp (*flag* tag) flanking homology arms along with previously tested sgRNAs (Figure 3F, Figure S1B, and Figure S2A). We then used PCR to amplify the genomic DNA sequence from F1 rollers and restriction analysis to identify F1 heterozygotes carrying the desired insertion (Figure 3G, Figure S2, B and C). These studies identified two K68A HR events among 93 F1 rollers (60 injected worms) and three *flag* HR events among 84 F1 rollers (40 injected worms) (data not shown). A similar PCR-detection strategy was used to introduce *mcherry* into the gene *vet-2*. In this experiment, mCherry expression was not visible in adult F1 rollers, but was easily detected among the F2 embryos produced by PCR-positive animals (Figure 3E). Taken together these findings show that CRISPR-Cas9-mediated HR occurs at a remarkably high frequency in *C. elegans*.

We compared the expression and localization of GFP::PIE-1 protein in our newly generated *gfp*::*pie-1* knock-in strains to strains in which *gfp*::*pie-1* was inserted at a heterologous site in the genome by MosSCI (Frokjaer-Jensen *et al.* 2008; Shirayama *et al.* 2012). The knock-in strains showed the expected localization of PIE-1 in two- to four-cell embryos (Figure 3C). Strikingly, immunoblot analysis using the PIE-1 monoclonal antibody (P4G5) revealed that GFP::PIE-1 protein was expressed at a much higher level in the CRISPR-Cas9-induced knock-in strains, similar to the expression level of endogenous PIE-1 protein (Figure 3D). These results are consistent with a previous study (Dickinson *et al.* 2013) and indicate, perhaps not surprisingly, that insertion of GFP into the endogenous locus can achieve near optimal expression levels of the tagged protein.

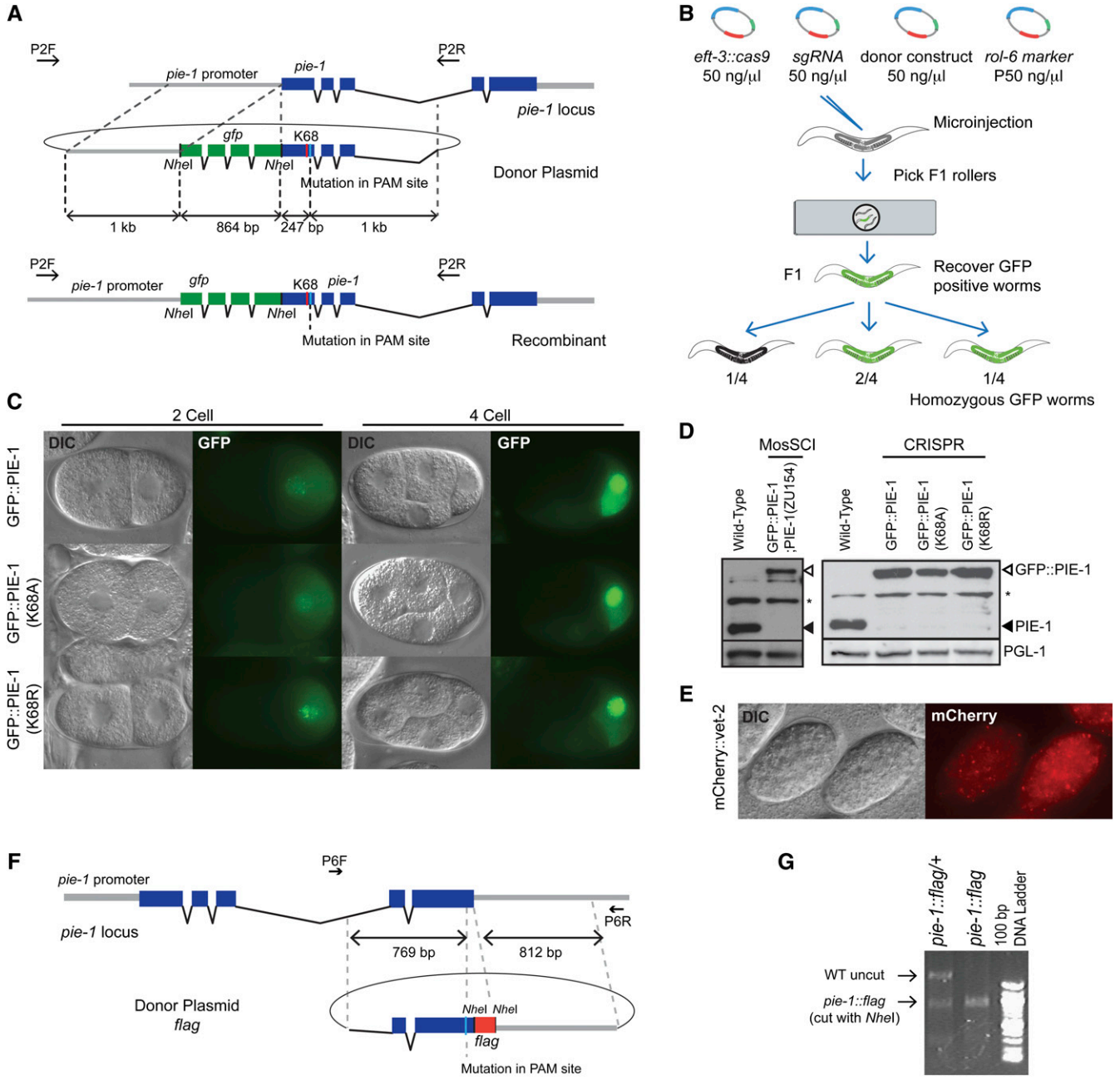

Figure 3 HR-mediated knock-in to generate fusion genes at endogenous loci. (A) Schematic of the Cas9/sgRNA target site and the donor plasmid for *gfp*::*pie-1* knock-ins. The donor plasmid contains the *gfp* coding sequence inserted immediately after the start codon of *pie-1*, 1 kb of homology flanking the CRISPR-Cas9 cleavage site, and a silent mutation in the PAM site. (B) Strategy to screen for *gfp* knock-in lines. We placed three F1 rollers at a time on a 2% agar pad and screened for GFP expression using epifluorescence microscopy. GFP-expressing worms were individually recovered and allowed to make F2 progeny for 1 day before being lysed for PCR and DNA sequence analysis. We confirmed Mendelian inheritance of *gfp* knock-in alleles among F2 progeny. (C) GFP::PIE-1 expression in the germline of two- to four-cell embryos of *gfp*::*pie-1* knock-in strains. (D) Immunoblot analysis showing PIE-1 expression levels in wild-type animals, MosSCI-mediated *gfp*::*pie-1* knock-in animals, and CRISPR-Cas9-mediated *gfp* knock-in animals. A MosSCI strain of *gfp*::*pie-1*; *pie-1(zu154)* was obtained by crossing *gfp*::*pie-1* (LGII) with the *pie-1(zu154)* (LGIII) null mutant. (E) mCherry expression in late embryos of the *mCherry*::*vet-2* knock-in strain. (F) Schematic of Cas9/sgRNA target sequence, PAM site, and donor plasmid for *pie-1*::*flag* knock-in. The PAM is located in the last exon of *pie-1*. The donor plasmid includes *flag* coding sequence immediately before the *pie-1* stop codon and ~800-bp homology arms flanking the target site. (G) PCR and restriction analysis of an HR event. PCR products were generated using the primers indicated in F, and the products were digested with *Nhe*I. The *pie-1*::*flag* gene conversion introduces an *Nhe*I RFLP that is observed in F1 heterozygous and F2 homozygous *pie-1*::*flag* animals.

Table 1 Co-CRISPR strategy for HR events

HR donor/targeted gene	No. injected	F1 rollers producing F2 twitchers/total F1 rollers	F1 having both rolling and twitching phenotype	F1 twitchers	F1 Twitcher-based HR frequency	Roller-based HR frequency	Roller producing F2 twitchers-based HR frequency
flag::*vet-2*/*vet-2*	40	29/65	0	62	2/62 (3%)	4/65 (6%)	3/29 (10%)
pie-1::*gfp*/*pie-1*	40	4/145	0	7	0/7 (0%)	7/145 (5%)	2/4 (50%)
smo-1::*flag*/*smo-1*	40	12/55	10	22	1/22 (5%)	1/55 (2%)	1/12 (8%)

Co-CRISPR for identifying HR events

Most of the HR work described above was performed before we realized the utility of Co-CRISPR markers for validating sgRNAs. To determine if the Co-CRISPR strategy could facilitate recovery of HR events, we co-injected *unc-22* sgRNAs along with CRISPR HR injection mixes targeting *vet-2*, *pie-1*, and *smo-1* genes (Figure S3). The findings from these studies suggest that using a Co-CRISPR marker can increase the frequency of HR events in the range of approximately two- to fourfold over those observed by first selecting F1 roller animals (Table 1). Interestingly, however, these studies required a modification to the Co-CRISPR screening strategy. For testing sgRNAs using Co-CRISPR, we found that F1 and F2 twitchers were equally likely to exhibit co-induction of indels with the second sgRNA. However, our data suggest that HR events were not enriched and might be depleted among nonrolling, F1 twitcher animals. One possible explanation for this surprising finding is that Cas9–sgRNA complexes may assemble in the germline cytoplasm and then segregate into maturing oocytes independently of the co-injected DNA (including both the roller DNA and of course the donor DNA plasmids). Zygotes inheriting programmed Cas9 could undergo NHEJ, but HR-directed repair would not be possible without the donor vector. Consistent with this reasoning, we found that in most cases HR events were enriched only among F1 animals that were both rolling, and thus had inherited the injected DNA, and also segregated twitching progeny, indicating that Cas9 was active (Table 1). For example among 145 F1 rollers, we found seven animals heterozygous for a 3′ insertion of *gfp* into the *pie-1* locus. Among the F1 twitchers that were nonrolling, zero were GFP positive, while among the 4 F1 rollers that segregated twitching progeny, 2 (50%) were GFP positive. One convenient aspect of searching for HR events among F1 rollers heterozygous for *unc-22* twitchers was that the unlinked twitcher phenotype could easily be segregated away in subsequent generations. These findings suggest that Co-CRISPR screening can enhance the detection of HR events. Indeed, we always found at least one HR event among the F1 rollers with twitcher progeny (3/29, 2/4, and 1/12). However, in most cases additional HR events were also recovered by scoring all the F1 rollers (Table 1).

A selection/counterselection strategy for recovering HR events

The above findings demonstrate that selections are not necessary for identifying and recovering HR events using the CRISPR-Cas9 system. However, for some experiments a dominant selection could save considerable time and expense, especially where insertion of heterologous DNA is likely to be tolerated, for example, when generating a null allele of a gene or when one wishes to precisely delete noncoding genes or regulatory elements. The inserted marker also has the potential benefit of providing a selection for maintaining strains that may not be homozygous viable. Previous studies have described several selection strategies, including *unc-119*, NeomycinR, PuromycinR, and HygromycinR (Frokjaer-Jensen *et al.* 2008; Giordano-Santini *et al.* 2010; Semple *et al.* 2010; Frokjaer-Jensen *et al.* 2012; Radman *et al.* 2013). To test a selection/counterselection scheme for CRISPR-induced HR, we decided to employ the *unc-119(+)* marker as well as a new worm antibiotic-resistance marker expressing the bacterial *BSD* gene as selectable markers and the *avr-15* gene as a counterselectable marker. We have previously shown that introducing an *avr-15(+)* plasmid into extrachromosomal arrays and balancer chromosomes can be used to facilitate their counterselection by growth on ivermectin (Duchaine *et al.* 2006; Shirayama *et al.* 2012). This counterselection can be thus used to remove *Cbr-unc-119(+)* or *BSD(+)* extrachromosomal transgenes, thereby facilitating the recovery of animals bearing an HR-induced insertion of the selectable marker. This counterselection approach requires a starting strain resistant to ivermectin, which is conferred by lesions in both the *avr-14* and *avr-15* genes. Ivermectin-resistant double-mutant strains are essentially wild type in appearance, and *Cbr-unc-119* ivermectin-resistant strains are available, or as noted above, new strains can readily be rendered ivermectin resistant by simply co-injecting sgRNAs targeting *avr-14* and *avr-15* (Figure 2).

To test this selection/counterselection strategy we first designed a donor plasmid containing the *BSD* gene flanked with 1-kb *pie-1* homology arms (Figure 4A). We injected 58 ivermectin-resistant animals with a mix containing this donor plasmid along with a validated *pie-1* sgRNA vector, the *Peft-3*::*Cas9* vector, the *rol-6* vector, and the *avr-15(+)* vector. Gravid F1 rollers were then placed ~11 per plate directly onto plates containing both blasticidin and ivermectin (Figure 4B; see *Materials and Methods*). After 3–4 days we found that 3 of 14 plates produced blasticidin-resistant, fertile animals (Figure 4B). In a second experiment, we injected the same injection mixture into 40 animals and obtained 103 F1 rollers, from which we identified four blasticidin-resistant strains. In each case, the desired HR events were confirmed both by phenotype and DNA sequence analysis (data not shown).

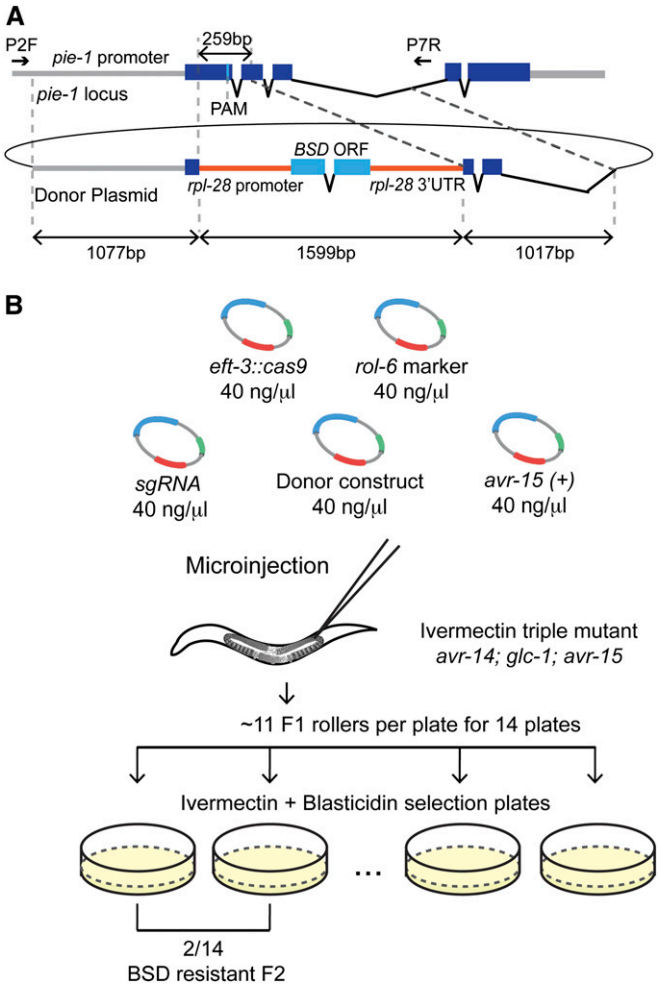

Figure 4 A blasticidin-resistance marker to select *pie-1* knockout mutants. (A) Schematic of the Cas9/sgRNA target sequence and an HR donor plasmid in which a heterologous blasticidin-resistance (*BSD*) gene replaces a region of *pie-1* and is flanked by 1-kb homology arms. The *BSD* gene is under the control of the *rpl-28* promoter (568 bp) and 3′-UTR (568 bp). (B) Schematic of the blasticidin selection strategy to precisely delete the *pie-1* gene. *pie-1a* sgRNA was co-injected with the Cas9 expression vector, the *rol-6* transformation marker, the *pie-1*Δ::*BSD* donor construct, and the *pCCM416*::*Pmyo-2*::*avr-15(+)* counterselection vector. The indicated number of F1 rollers was transferred to the plates containing 2 ng/ml ivermectin to select against the extrachromosomal array and 100 μg/ml blasticidin to identify *BSD* knock-in lines. We identified two plates with resistant, fertile adults among 14 plates, 3–4 days after transferring animals.

We also tested *Cbr-unc-119(+)* as a selectable marker in this selection/counterselection assay. For this experiment we sought to enlarge an *oma-1* deletion (*tm1396*), replacing the *oma-1* promoter, coding region, and 3′UTR with the *cb-unc-119*(+) gene flanked by *loxP* sites (Dickinson *et al.* 2013) (Figure S4). We injected 15 ivermectin-resistant *Cbr-unc-119*; *oma-1(tm1396)* animals with a mix containing *oma-1* sgRNA, *Cbr-unc-119(+)* oma-1 gene replacement donor vector, a heat-shock Cas9 vector, the *rol-6* vector, and the *avr-15(+)* vector. Injected animals were allowed to recover for 2 hr after injection and were then heat shocked at 34° for 1.5 hr (Waaijers *et al.* 2013). Gravid non-Unc F1 rollers were collected 15 per plate on six plates, and each population was subjected to ivermectin counterselection. After 4 days, one of the six plates produced healthy ivermectin resistant non-Unc-119 nonrolling animals. Insertion of the *Cbr-unc-119* vector and deletion of the *oma-1* sequences was confirmed by PCR (data not shown).

Optimizing sgRNA and donor molecule selection

There is much work still to do to optimize CRISPR methodology for *C. elegans*. For example, it remains unclear at this point why upward of half of the sgRNAs tested fail to induce events. The sgRNAs that we have tested and the activities observed are summarized in Table S1, and all of the active sgRNA vectors will be made available (through Addgene). Another area requiring more study is how best to optimize HR donors. All of the HR donor molecules used in the experiments described here were circular plasmids with at least 300-bp homology arms (Figure S2A). For GFP insertion we used either 800-bp or 1-kb homology arms and observed roughly equal frequencies of HR in both cases (Figure 3A and Figure S3B). Future studies should explore shorter homology arms and other types of donor molecules including linear dsDNA donor molecules produced, for example, by PCR, as well as chemically synthesized ssDNA. It will also be important to explore the optimal distance between the cut site and the homology arm. Increasing this distance requires longer gene-conversion tracts and in other organisms is correlated with reduced frequency of the desired homologous event (Paques and Haber 1999). Our findings suggest that gene-conversion tracts of ~250 bp are common in *C. elegans*. Optimizing HR conditions for each type of donor molecule will likely require extensive experimentation to generate statistically significant findings on relative efficiencies. Although there is still much work to do, the efficiencies reported here are already remarkably high. For example, indels were frequently identified in >10% of F1 rollers, and the ratio of HR events to the total number of CRISPR-Cas9-induced-repair events was consistently ~10% in experiments where both HR and indels were monitored.

Our findings provide a versatile framework for using CRISPR-Cas9 genome editing in *C. elegans*, and the Co-CRISPR strategy we employ is likely to be of value for CRISPR-Cas9 studies in other organisms. The tools described here, however, are likely to be just the beginning of what will be possible in the near future. For example, the use of catalytically inactive Cas9 fusion proteins to tether regulators to DNA targets has not been described yet in *C. elegans*, but it is already finding many exciting applications in other systems (Cheng *et al.* 2013; Larson *et al.* 2013; Mali *et al.* 2013a; Qi *et al.* 2013; Kearns *et al.* 2014). CRISPR-Cas9 technology should also dramatically facilitate the use of other nematode models, including species distantly related to *Caenorhaditis elegans* and perhaps parasitic nematodes. The ability to efficiently engineer genomes will only enhance

the utility of model organisms where gene variants can now be generated and analyzed rapidly and cost effectively, facilitating the production of new animals models for human disease-associated alleles. Moreover, CRISPR-Cas9-engineered strains with special alleles of important genes can be used as starting strains in forward genetic screens, including suppressor and enhancer screens, which are extremely powerful in *C. elegans*. It is now easier than ever for researchers to use *C. elegans* to explore the function of conserved genes of interest. Indeed, the CRISPR-Cas9 technology lowers the barrier to move from one system to another, effectively making all organisms one, when exploring conserved cellular mechanisms.

Acknowledgments

We thank John Calarco for sharing information and materials prior to publication and Wen Tang for building *Phsp*::*Cas9* plasmid. We are grateful to members of the Mello and Ambros labs for input and discussion. M. Seth is a Howard Hughes Medical Institute International Student Research Fellow. This work was supported by a National Institutes of Health grant (GM058800) to C.C.M. C.C.M. is a Howard Hughes Medical Institute Investigator.

Literature Cited

Bassett, A. R., C. Tibbit, C. P. Ponting, and J. L. Liu, 2013 Highly efficient targeted mutagenesis of Drosophila with the CRISPR/Cas9 system. Cell Rep. 4: 220–228.

Benian, G. M., S. W. L'Hernault, and M. E. Morris, 1993 Additional sequence complexity in the muscle gene, unc-22, and its encoded protein, twitchin, of *Caenorhabditis elegans*. Genetics 134: 1097–1104.

Bhaya, D., M. Davison, and R. Barrangou, 2011 CRISPR-Cas systems in bacteria and archaea: versatile small RNAs for adaptive defense and regulation. Annu. Rev. Genet. 45: 273–297.

Brenner, S., 1974 The genetics of *Caenorhabditis elegans*. Genetics 77: 71–94.

Chang, N., C. Sun, L. Gao, D. Zhu, X. Xu *et al.*, 2013 Genome editing with RNA-guided Cas9 nuclease in zebrafish embryos. Cell Res. 23: 465–472.

Chen, C., L. A. Fenk, and M. de Bono, 2013 Efficient genome editing in *Caenorhabditis elegans* by CRISPR-targeted homologous recombination. Nucleic Acids Res. 41: e193.

Cheng, A. W., H. Wang, H. Yang, L. Shi, Y. Katz *et al.*, 2013 Multiplexed activation of endogenous genes by CRISPR-on, an RNA-guided transcriptional activator system. Cell Res. 23: 1163–1171.

Chiu, H., H. T. Schwartz, I. Antoshechkin, and P. W. Sternberg, 2013 Transgene-free genome editing in *Caenorhabditis elegans* using CRISPR-Cas. Genetics 195: 1167–1171.

Cho, S. W., S. Kim, J. M. Kim, and J. S. Kim, 2013a Targeted genome engineering in human cells with the Cas9 RNA-guided endonuclease. Nat. Biotechnol. 31: 230–232.

Cho, S. W., J. Lee, D. Carroll, J. S. Kim, and J. Lee, 2013b Heritable gene knockout in *Caenorhabditis elegans* by direct injection of Cas9-sgRNA ribonucleoproteins. Genetics 195: 1177–1180.

Cong, L., F. A. Ran, D. Cox, S. Lin, R. Barretto *et al.*, 2013 Multiplex genome engineering using CRISPR/Cas systems. Science 339: 819–823.

Dent, J. A., M. M. Smith, D. K. Vassilatis, and L. Avery, 2000 The genetics of ivermectin resistance in *Caenorhabditis elegans*. Proc. Natl. Acad. Sci. USA 97: 2674–2679.

Dicarlo, J. E., A. J. Conley, M. Penttila, J. Jantti, H. H. Wang *et al.*, 2013 Yeast Oligo-Mediated Genome Engineering (YOGE). ACS Synth Biol 2: 741–749.

Dickinson, D. J., J. D. Ward, D. J. Reiner, and B. Goldstein, 2013 Engineering the *Caenorhabditis elegans* genome using Cas9-triggered homologous recombination. Nat. Methods 10: 1028–1034.

Duchaine, T. F., J. A. Wohlschlegel, S. Kennedy, Y. Bei, D. Conte, Jr. *et al.*, 2006 Functional proteomics reveals the biochemical niche of *C. elegans* DCR-1 in multiple small-RNA-mediated pathways. Cell 124: 343–354.

Feng, Z., Y. Mao, N. Xu, B. Zhang, P. Wei *et al.*, 2014 Multigeneration analysis reveals the inheritance, specificity, and patterns of CRISPR/Cas-induced gene modifications in Arabidopsis. Proc. Natl. Acad. Sci. USA 111: 4632–4637.

Feng, Z., B. Zhang, W. Ding, X. Liu, D. L. Yang *et al.*, 2013 Efficient genome editing in plants using a CRISPR/Cas system. Cell Res. 23: 1229–1232.

Friedland, A. E., Y. B. Tzur, K. M. Esvelt, M. P. Colaiacovo, G. M. Church *et al.*, 2013 Heritable genome editing in *C. elegans* via a CRISPR-Cas9 system. Nat. Methods 10: 741–743.

Frokjaer-Jensen, C., M. W. Davis, C. E. Hopkins, B. J. Newman, J. M. Thummel *et al.*, 2008 Single-copy insertion of transgenes in *Caenorhabditis elegans*. Nat. Genet. 40: 1375–1383.

Frokjaer-Jensen, C., M. W. Davis, M. Ailion, and E. M. Jorgensen, 2012 Improved Mos1-mediated transgenesis in *C. elegans*. Nat. Methods 9: 117–118.

Gilbert, L. A., M. H. Larson, L. Morsut, Z. Liu, G. A. Brar *et al.*, 2013 CRISPR-mediated modular RNA-guided regulation of transcription in eukaryotes. Cell 154: 442–451.

Giordano-Santini, R., S. Milstein, N. Svrzikapa, D. Tu, R. Johnsen *et al.*, 2010 An antibiotic selection marker for nematode transgenesis. Nat. Methods 7: 721–723.

Gratz, S. J., A. M. Cummings, J. N. Nguyen, D. C. Hamm, L. K. Donohue *et al.*, 2013 Genome engineering of *Drosophila* with the CRISPR RNA-guided Cas9 nuclease. Genetics 194: 1029–1035.

Grishok, A., and C. C. Mello, 2002 RNAi (Nematodes: *Caenorhabditis elegans*). Adv. Genet. 46: 339–360.

Hannon, G. J., 2002 RNA interference. Nature 418: 244–251.

Horii, T., S. Morita, M. Kimura, R. Kobayashi, D. Tamura *et al.*, 2013 Genome engineering of mammalian haploid embryonic stem cells using the Cas9/RNA system. Peer J. 1: e230.

Horvath, P., and R. Barrangou, 2010 CRISPR/Cas, the immune system of bacteria and archaea. Science 327: 167–170.

Jiang, W., D. Bikard, D. Cox, F. Zhang, and L. A. Marraffini, 2013 RNA-guided editing of bacterial genomes using CRISPR-Cas systems. Nat. Biotechnol. 31: 233–239.

Jinek, M., K. Chylinski, I. Fonfara, M. Hauer, J. A. Doudna *et al.*, 2012 A programmable dual-RNA-guided DNA endonuclease in adaptive bacterial immunity. Science 337: 816–821.

Katic, I., and H. Grosshans, 2013 Targeted heritable mutation and gene conversion by Cas9-CRISPR in *Caenorhabditis elegans*. Genetics 195: 1173–1176.

Kearns, N. A., R. M. Genga, M. S. Enuameh, M. Garber, S. A. Wolfe *et al.*, 2014 Cas9 effector-mediated regulation of transcription and differentiation in human pluripotent stem cells. Development 141: 219–223.

Larson, M. H., L. A. Gilbert, X. Wang, W. A. Lim, J. S. Weissman *et al.*, 2013 CRISPR interference (CRISPRi) for sequence-specific control of gene expression. Nat. Protoc. 8: 2180–2196.

Lo, T. W., C. S. Pickle, S. Lin, E. J. Ralston, M. Gurling *et al.*, 2013 Precise and heritable genome editing in evolutionarily diverse nematodes using TALENs and CRISPR/Cas9 to engineer insertions and deletions. Genetics 195: 331–348.

Ma, Y., B. Shen, X. Zhang, Y. Lu, W. Chen *et al.*, 2014 Heritable multiplex genetic engineering in rats using CRISPR/Cas9. PLoS ONE 9: e89413.

Mali, P., J. Aach, P. B. Stranges, K. M. Esvelt, M. Moosburner *et al.*, 2013a CAS9 transcriptional activators for target specificity screening and paired nickases for cooperative genome engineering. Nat. Biotechnol. 31: 833–838.

Mali, P., L. Yang, K. M. Esvelt, J. Aach, M. Guell *et al.*, 2013b RNA-guided human genome engineering via Cas9. Science 339: 823–826.

Mello, C. C., C. Schubert, B. Draper, W. Zhang, R. Lobel *et al.*, 1996 The PIE-1 protein and germline specification in *C. elegans* embryos. Nature 382: 710–712.

Moerman, D. G., and D. L. Baillie, 1979 Genetic organization in *Caenorhabditis elegans*: fine-structure analysis of the unc-22 gene. Genetics 91: 95–103.

Paques, F., and J. E. Haber, 1999 Multiple pathways of recombination induced by double-strand breaks in *Saccharomyces cerevisiae*. Microbiol. Mol. Biol. Rev. 63: 349–404.

Qi, L. S., M. H. Larson, L. A. Gilbert, J. A. Doudna, J. S. Weissman *et al.*, 2013 Repurposing CRISPR as an RNA-guided platform for sequence-specific control of gene expression. Cell 152: 1173–1183.

Radman, I., S. Greiss, and J. W. Chin, 2013 Efficient and rapid *C. elegans* transgenesis by bombardment and hygromycin B selection. PLoS ONE 8: e76019.

Ran, F. A., P. D. Hsu, C. Y. Lin, J. S. Gootenberg, S. Konermann *et al.*, 2013 Double nicking by RNA-guided CRISPR Cas9 for enhanced genome editing specificity. Cell 154: 1380–1389.

Ren, X., J. Sun, B. E. Housden, Y. Hu, C. Roesel *et al.*, 2013 Optimized gene editing technology for *Drosophila melanogaster* using germ line-specific Cas9. Proc. Natl. Acad. Sci. USA 110: 19012–19017.

Semple, J. I., R. Garcia-Verdugo, and B. Lehner, 2010 Rapid selection of transgenic *C. elegans* using antibiotic resistance. Nat. Methods 7: 725–727.

Shirayama, M., M. Seth, H. C. Lee, W. Gu, T. Ishidate *et al.*, 2012 piRNAs initiate an epigenetic memory of nonself RNA in the *C. elegans* germline. Cell 150: 65–77.

Sternberg, S. H., S. Redding, M. Jinek, E. C. Greene, and J. A. Doudna, 2014 DNA interrogation by the CRISPR RNA-guided endonuclease Cas9. Nature 507: 62–67.

Terns, M. P., and R. M. Terns, 2011 CRISPR-based adaptive immune systems. Curr. Opin. Microbiol. 14: 321–327.

Tzur, Y. B., A. E. Friedland, S. Nadarajan, G. M. Church, J. A. Calarco *et al.*, 2013 Heritable custom genomic modifications in *Caenorhabditis elegans* via a CRISPR-Cas9 system. Genetics 195: 1181–1185.

Voinnet, O., 2001 RNA silencing as a plant immune system against viruses. Trends Genet. 17: 449–459.

Waaijers, S., V. Portegijs, J. Kerver, B. B. Lemmens, M. Tijsterman *et al.*, 2013 CRISPR/Cas9-targeted mutagenesis in *Caenorhabditis elegans*. Genetics 195: 1187–1191.

Wang, H., H. Yang, C. S. Shivalila, M. M. Dawlaty, A. W. Cheng *et al.*, 2013 One-step generation of mice carrying mutations in multiple genes by CRISPR/Cas-mediated genome engineering. Cell 153: 910–918.

Wang, T., J. J. Wei, D. M. Sabatini, and E. S. Lander, 2014 Genetic screens in human cells using the CRISPR-Cas9 system. Science 343: 80–84.

Wiedenheft, B., S. H. Sternberg, and J. A. Doudna, 2012 RNA-guided genetic silencing systems in bacteria and archaea. Nature 482: 331–338.

Yu, Z., H. Chen, J. Liu, H. Zhang, Y. Yan *et al.*, 2014 Various applications of TALEN- and CRISPR/Cas9-mediated homologous recombination to modify the Drosophila genome. Biol Open 3: 271–280.

Zamore, P. D., 2001 RNA interference: listening to the sound of silence. Nat. Struct. Biol. 8: 746–750.

Zhao, P., Z. Zhang, H. Ke, Y. Yue, and D. Xue, 2014 Oligonucleotide-based targeted gene editing in *C. elegans* via the CRISPR/Cas9 system. Cell Res. 24: 247–250.

Zhou, J., B. Shen, W. Zhang, J. Wang, J. Yang *et al.*, 2014 One-step generation of different immunodeficient mice with multiple gene modifications by CRISPR/Cas9 mediated genome engineering. Int. J. Biochem. Cell Biol. 46: 49–55.

Communicating editor: O. Hobert

GENETICS

Supporting Information
http://www.genetics.org/lookup/suppl/doi:10.1534/genetics.114.166389/-/DC1

A Co-CRISPR Strategy for Efficient Genome Editing in *Caenorhabditis elegans*

Heesun Kim, Takao Ishidate, Krishna S. Ghanta, Meetu Seth, Darryl Conte Jr., Masaki Shirayama, and Craig C. Mello

DOI: 10.1534/genetics.114.166389

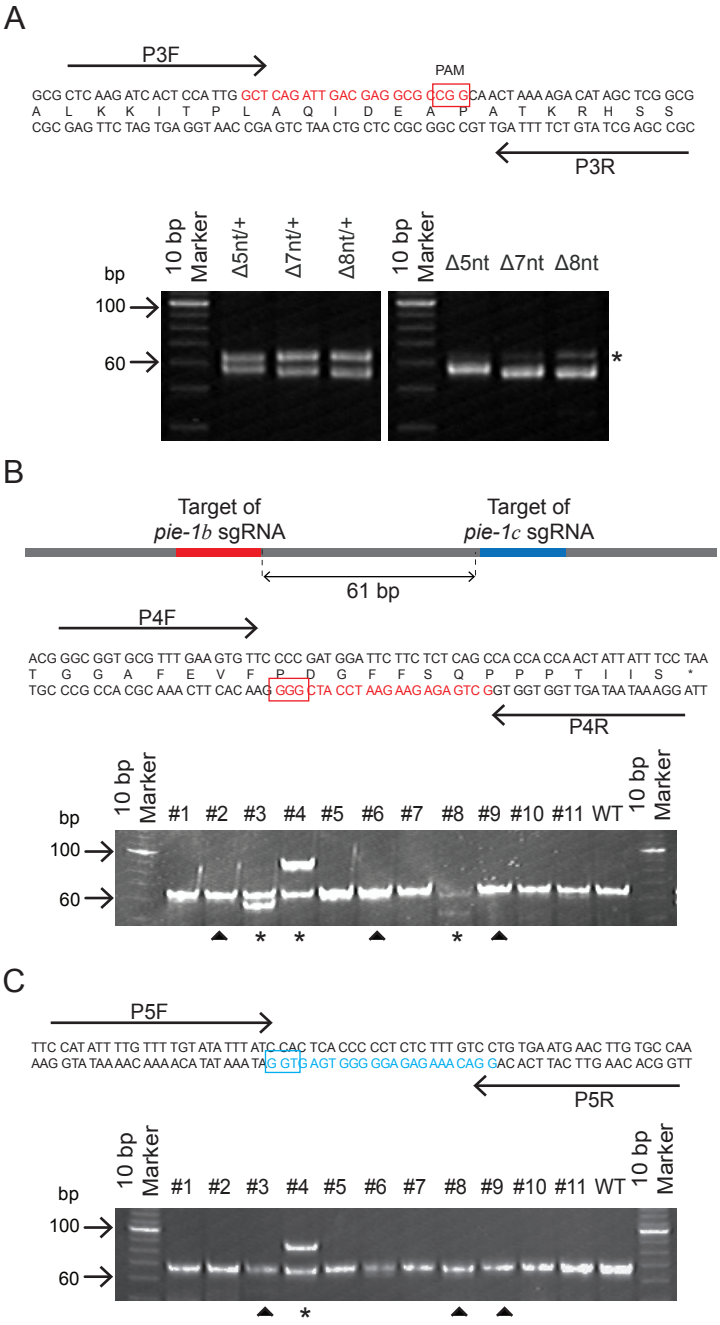

Figure S1. Detecting small indels on 15% polyacrylamide gels. (A) The indicated primers (arrows) were used to amplify sequences immediately surrounding the CRISPR-Cas9 target site (red). The indels in this experiment were from an HR experiment, so an initial PCR was performed using primers outside of the homology arms of the donor template (Figure S2A). The initial PCR was used as a template to amplify the target site using the indicated primers. PCR products from F1 heterozygotes (left) and F2 homozygotes (right) were separated on a non-denaturing 15% polyacrylamide gel and stained with ethidium bromide. The asterisk indicates the PCR product amplified from residual donor plasmids in the single worm lysate (B) and (C) Test of two uncharacterized *pie-1* sgRNAs using the Co-CRISPR strategy and PAGE analysis. The *pie-1* sgRNA vectors were combined and co-injected with the *unc-22* sgRNA, Cas9, and *rol-6* plasmids. The *pie-1* sgRNA target sites (shown in red and blue) are separated by 61 bp. As this experiment did not include an HR donor, only a single round of PCR was performed with the indicated primers (arrows). We lysed 11 F1 animals with the twitching phenotype (#3, #8, and #9-11) or that produced twitching progeny (#1-2 and #4-7). WT, wild type N2 genomic DNA was used as a template. Asterisks indicate lanes in which small indels were detected. The filled triangles indicate lanes in which the primer pair could not detect the indels.

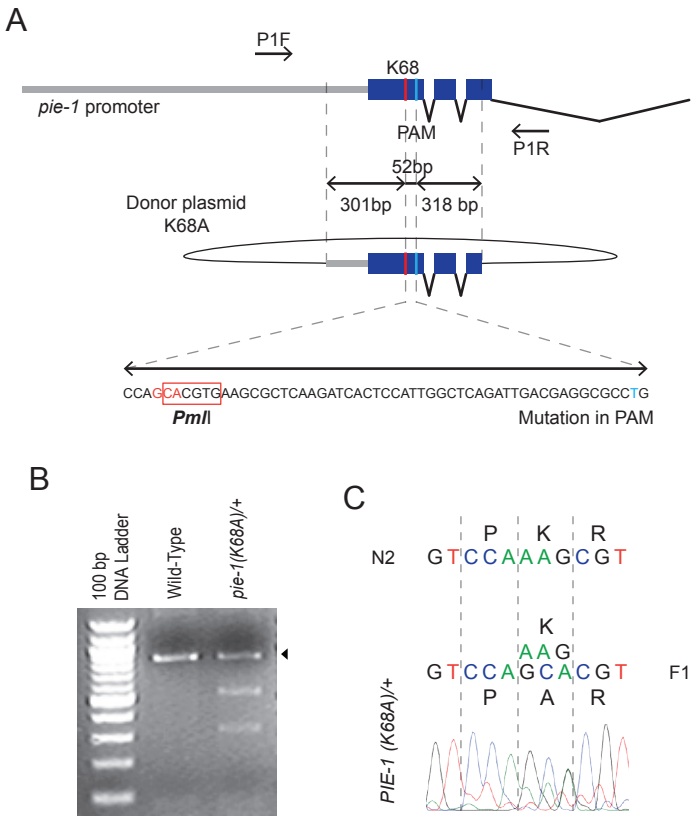

Figure S2. Site-specific mutagenesis of *pie-1* by HR. (A) Schematic of the Cas9/sgRNA target sites in *pie-1* locus and donor plasmids. The K68A donor plasmid contains ~300 bp of homology flanking the 52 bp target region between the K68 codon and PAM site and introduces a *Pml*I restriction site (red box). The PAM site of each donor was disrupted by silent mutations so that it will not be targeted by CRISPR-Cas9. The blue bar indicates the PAM site, and the red bar indicates the position of K68. (B) PCR and restriction enzyme analysis of wild type control worms and F1 rollers from K68A CRISPR-Cas9-mediated HR experiments. PCR primers outside of the donor homology arms (P1F and P1R for K68A) are indicated in (A). Restriction analysis following PCR shows the RFLP in *pie-1(K68A)/+*. The wild type product is indicated by the filled triangle. (C) DNA sequence analyses to confirm the desired point mutations. Note that the PCR products for sequencing were amplified using the primers outside of donor plasmid, as indicated in (A).

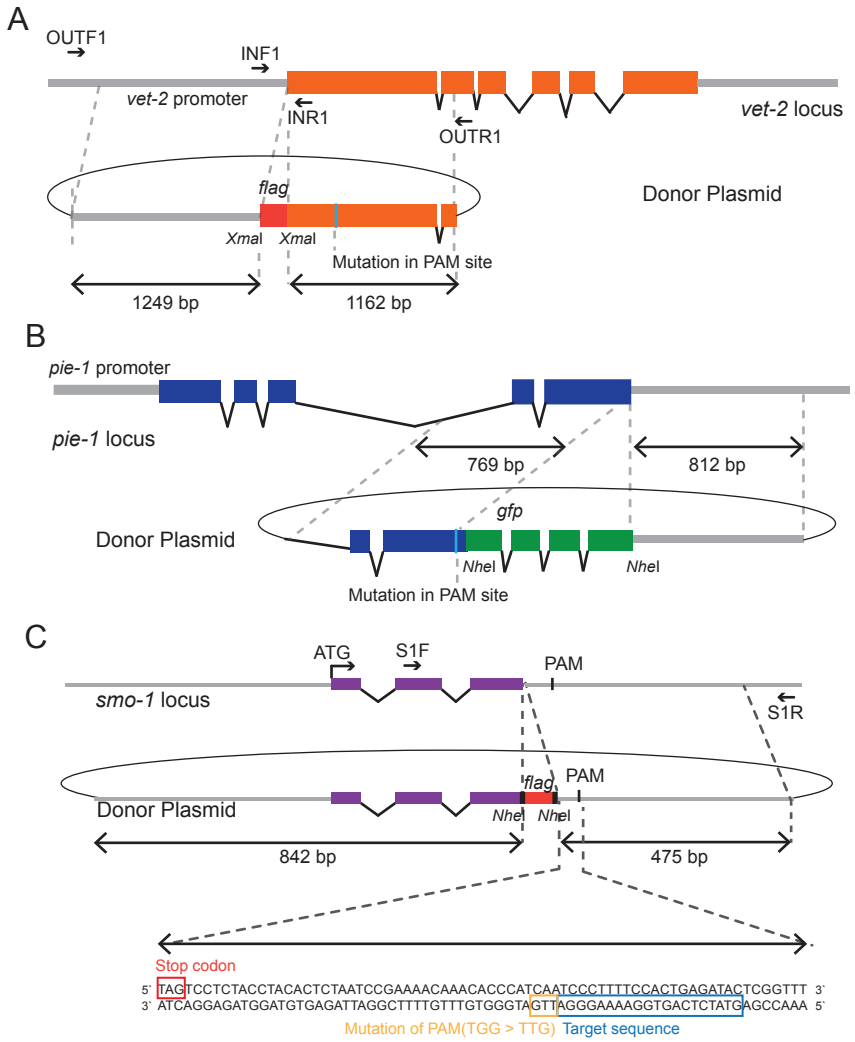

Figure S3. HR donor plasmids used in Co-CRISPR experiments. (A) Schematic of the *flag::vet-2* donor plasmid. The *flag* coding sequence was inserted immediately after the *vet-2* start codon and flanked by ~1200 bp homology arms. (B) Schematic of the *pie-1::gfp* donor plasmid. (C) Schematic of the *smo-1::flag* donor plasmid. The donor plasmid includes *flag* coding sequence immediately before the *smo-1* stop codon and asymmetrical homology arms (~800 bp and ~500 bp) flanking the target site, and the Cas9/sgRNA target sequence is located in the 3'UTR of *smo-1*. The PAM sites mutated in each donor indicate the locations of the Cas9/sgRNA target sites.

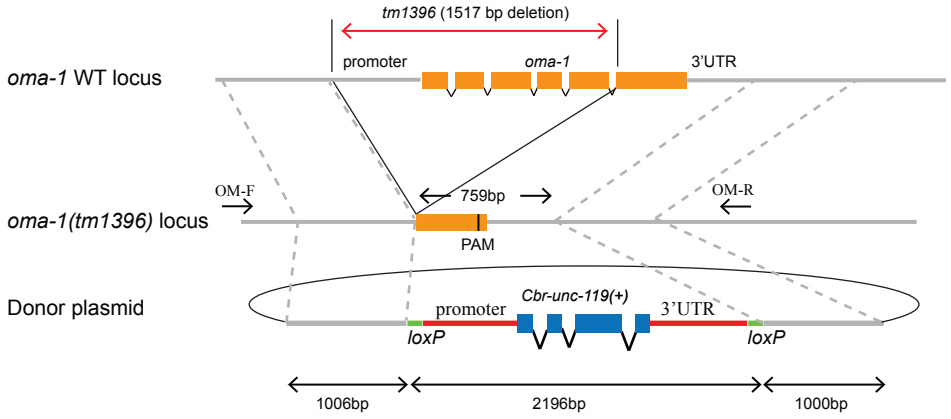

Figure S4. Selection/counterselection experiment to delete the entire *oma-1(tm1396)* locus. Schematic of the Cas9/sgRNA target site and the donor plasmid containing *Cbr-unc-119(+)* flanked by *loxP* sites and 1 kb homology arms. The indicated primers OM-F and OM-R were used for PCR analysis.

Table S1. Summary of sgRNAs sequences and their efficiency

Name	Sequence	S/AS	% efficiency
avr-14 no.1	GAATATTGAAAGACTATGAT(TGG)	S	10
avr-14 no.2	GATTGGAGAGTTAGACCACG(TGG)	S	20
avr-15 no.9	GCAGAAAATGAATGTCATAC(AGG)	AS	HIGH
avr-15 no.10	GTTTGCAATATAAGTCACCC(AGG)	AS	HIGH
unc-22 no.2	GAACCCGTTGCCGAATACAC(AGG)	S	5
unc-22 no.9	GCCTTTGCTTCGATTTTCTT(TGG)	AS	0
unc-4 no.1	GTTATCGTCATCCGGTGACG(TGG)	AS	10
rde-3 no.3	GAATTTGAGCTTGAACGAGC(TGG)	AS	LOW
rde-3 no.4	GTCGATACTTCAAAATTAAT(TGG)	AS	LOW
lon-2 no.1	GGGAAACTATACCCTCACTG(TGG)	S	30
dpy-11 no.2	GCAAGGATCTTCAAAAAGCA(CGG)	S	0.4
dpy-11 no.4	GATGCTTGTAGTCTGGAACT(GGG)	AS	
unc-32 no.1	GATAGGAAGCATCAGATTGA(AGG)	AS	0
unc-32 no.2	GTTGCTGAACTGGGAGAGCT(CGG)	S	
bli-2 no.1	GGATTTGCTGCTACTGAATC(CGG)	AS	0
bli-2 no.2	GATGGACGGGATGGTAGAGA(TGG)	S	
dpy-5 no.2	GTCGGATTCGGCGCTGCATG(CGG)	S	0
dpy-5 no.3	GGTTTCCTGGAGCTCCGGCT(GGG)	AS	
ben-1 no.3	GGATATCACTTCCCAGAACT(TGG)	AS	0
ben-1 no.5	GGGAGAAAGTGATTTGCAGT(TGG)	S	
pie-1 a	GGCTCAGATTGACGAGGCGC(CGG)	S	24
pie-1 b	GCTGAGAGAAGAATCCATCG(GGG)	AS	15
pie-1 c	GGACAAAGAGAGGGGGTGAG(TGG)	AS	7.5
pie-1 d	GTTGAGTGCAGCCATTTGCT(CGG)	AS	5
smo-1 a	GCCGATGATGCAGCTCAAGC(AGG)	S	LOW
smo-1 b	GTGCACTTCCGTGTAAAGTA(TGG)	S	HIGH
smo-1 c	GTCTACCAAGAGCAGCTGGG(CGG)	S	HIGH
smo-1 d	GTATCTCAGTGGAAAAGGGA(TGG)	S	HIGH
vet-2	GTTGGATCATAGGATACCGG(TGG)	AS	38
C35E7.6	GGGCACCATACCGAGTGATG(GGG)	AS	100
oma-1	GATCCAATGATGTCATGTAA(CGG)	S	LOW

Table S2. Summary of primer sequences for sgRNA plasmid generation

Name	Sequence
CMo16428	TGAATTCCTCCAAGAACTCG
CMo16429	AAGCTTCACAGCCGACTATG
sgRNA_F	G(N)19GTTTTAGAGCTAGAAATAGC
avr-14 sgRNA_F	GATTGGAGAGTTAGACCACGGTTTTAGAGCTAGAAATAGC
avr-15 sgRNA_F	GTTTGCAATATAAGTCACCCGTTTTAGAGCTAGAAATAGC
unc-22 sgRNA_F	GAACCCGTTGCCGAATACACGTTTTAGAGCTAGAAATAGC
pie-1 a sgRNA_F	GGCTCAGATTGACGAGGCGCGTTTTAGAGCTAGAAATAGC
pie-1 b sgRNA_F	GCTGAGAGAAGAATCCATCGGTTTTAGAGCTAGAAATAGC
pie-1 c sgRNA_F	GGACAAAGAGAGGGGGTGAGGTTTTAGAGCTAGAAATAGC
smo-1 sgRNA_F	GTATCTCAGTGGAAAAGGGAGTTTTAGAGCTAGAAATAGC
vet-2 sgRNA_F	GTTGGATCATAGGATACCGGGTTTTAGAGCTAGAAATAGC
oma-1 sgRNA F	GATCCAATGATGTCATGTAAGTTTTAGAGCTAGAAATAGC
sgRNA_R	(N)19CAAACATTTAGATTTGCAATTC
avr-14 sgRNA_R	CGTGGTCTAACTCTCCAATCAAACATTTAGATTTGCAATTC
avr-15 sgRNA_R	GGGTGACTTATATTGCAAACAAACATTTAGATTTGCAATTC
unc-22 sgRNA_R	GTGTATTCGGCAACGGGTTCAAACATTTAGATTTGCAATTC
pie-1 a sgRNA_R	GCGCCTCGTCAATCTGAGCCAAACATTTAGATTTGCAATTC
pie-1 b sgRNA_R	CGATGGATTCTTCTCTCAGCAAACATTTAGATTTGCAATTC
pie-1 c sgRNA_R	CTCACCCCCTCTCTTTGTCCAAACATTTAGATTTGCAATTC
smo-1 sgRNA_R	TCCCTTTTCCACTGAGATACAAACATTTAGATTTGCAATTC
vet-2 sgRNA_R	CCGGTATCCTATGATCCAACAAACATTTAGATTTGCAATTC
oma-1 sgRNA R	TTACATGACATCATTGGATCCAAACATTTAGATTTGCAATTC

Table S3. Summary of primer sequences for repair template and PCR screening

Name	Sequence
C_PIE-1 PF	ATAGCCCGATTTTGGAGGTG
C_PIE-1 PR	CCTCGAATTTTGGCAATTTTTC
C_PIE-1 301L	ATGGATTTCTCGCCGTTTTTTC
C_PIE-1 318R	GTTGTATCCACGTCGTCTCG
C_PIE-1(K68A)_F	GGAAAATGGCTTCGTCCAGCACGTGAAGCG
C_PIE-1(K68A)_R	CTTGAGCGCTTCACGTGCTGGACGAAGCC
C_PIE-1(K68R)_F	GGAAAATGGCTTCGTCCTAGGCGTGAAGCG
C_PIE-1(K68R)_R	CTTGAGCGCTTCACGCCTAGGACGAAGCC
C_PIE-1 a MF	GCTATGTCTTTTAGTTGCAGGCGCCTC
C_PIE-1 a MR	CAGATTGACGAGGCGCCTGCAACTAA
SMO-1 PF	CGATTTTTCGGCTCATTTCG
SMO-1 PR	CCTCGTCAAATCCGAAATCG
SMO MF	CACCCATCAATCCCTTTTC
SMO MR	GAAAAGGGATTGATGGGTG
P1F	GTTTTTGCCCCCAAATTC
P1R	TGATGCTTCGATGCTGAAGA
P2F	GGCGTCAAAAGACATATGTAAAAG
P2R	CGCAATGGATGATTTTTGTC
P3F	GCCGAGCTATGTCTTTTAG
P3R	CTCAAGATCACTCCATTGGC
P4F	GGCGGTGCGTTTGAAGTGT
P4R	GGAAATAATAGTTGGTGGTGGC
P5F	CCATATTTTGTTTTGTATATTTATC
P5R	GGCACAAGTTCATTCACAGG
P6F	GCGCAGCGAATTTTTGGGGT
P6R	TATCACAATTCTCTCCGTGC
P7R	CGGAGAACTTGCCAAAATGAAG
S1F	GAAGTGCACTTCCGTGTAAAGTATGGAACC
S1R	CCGGCTGCTATTTCATTGAT
MC. OUT F1 (vet-2)	GCTCAAGAAAGCCAATGGAG
MC. OUT R1 (vet-2)	TTCTGAACCAGTCGATGCAG
MC.IN F1 (vet-2)	ATGGAGGGATCTGTCAATGG
MC.IN R1 (vet-2)	TGGCAGTCGAGACACTTCAG
FL. IN F1 (vet-2)	CACAAAACCGGCCAAAAA
FL. IN R1 (vet-2)	TCGGTCTTGCAGAAACCAC
OM-F	CAACGTTTGCGTGTACAGAAG
OM-R	GGCTCACGTACGCAGCACTAC